Fast-neutron Induced Reactions at the nELBE Time-of-flight Facility

Junghans, A. R.; Beyer, R.; Elekes, Z.; Grosse, E.; Hannaske, R.; Koegler, T.;
Massarczyk, R.; Schwengner, R.; Wagner, A.;

Perma-Link to Publication Repository of HZDR:

https://www.hzdr.de/publications/Publ-21758

Fast-Neutron Induced Reactions at the nELBE Time-of-Flight Facility

A. R. Junghans,[1, *] R. Beyer,[1] Z. Elekes,[1] E. Grosse,[1, †] R. Hannaske,[1, †]
T. Kögler,[1, †] R. Massarczyk,[1, †] R. Schwengner,[1] and A. Wagner[1]

[1] *Helmholtz-Zentrum Dresden-Rossendorf, Postfach 510119, 01314 Dresden, Germany*
(Dated: January 10, 2014)

The compact neutron-time-of-flight facility nELBE at the superconducting electron accelerator ELBE of Helmholtz-Zentrum Dresden-Rossendorf is being rebuilt and extended with a low-background experimental hall. The neutron radiator consists of a liquid lead circuit without additional neutron moderators. The useful neutron spectrum extends from some tens of keV to about 10 MeV. nELBE is intended to deliver cross section data of fast-neutron nuclear interactions e.g. for the transmutation of nuclear waste and improvement of neutron physical simulations of innovative nuclear systems. Before the extension of the facility, the photon production cross section of ^{56}Fe was measured with an HPGe detector and the inelastic neutron scattering cross section to the first few excited states in ^{56}Fe was determined. The neutron total cross sections of Au and Ta were determined in the energy from 200 keV to 7 MeV in a transmission experiment.

I. INTRODUCTION

A new compact photo-neutron source using a superconducting electron accelerator is under construction at the Helmholtz-Zentrum Dresden-Rossendorf (HZDR). The time-of-flight path will be between 4 and 11 m. A much larger time-of-flight experimental hall allows us to reduce the background from scattered neutrons as all walls including ceiling and floor are at least 3 m away from the evacuated neutron beam line. The facility is dedicated to measurements in the fast neutron range. A compact liquid lead circuit is used as a neutron producing target. Through this technology the neutron beam intensity is not limited by the heat dissipation inside the target. The technical design including thermomechanical parameters of the liquid lead circuit and the beam dump is discussed in [1]. The neutron source strength at the nominal beam current has been calculated to be 10^{13} neutrons/s, [2]. The accelerator produces high brilliance beams with variable micropulse repetition rates and duty cycles. The electrons are accelerated up to 40 MeV in continuous wave-mode by superconducting radio frequency cavities. The maximum average beam current at a micropulse rate of 13 MHz is 1 mA. For typical time-of-flight measurements the repetition rate is reduced to 100-200 kHz. The bunch length is about 5 ps, so that the time-of-flight resolution is not degraded and short flight paths can be used with a high resolution detection system. Figure 1 shows the floor plan of the new neutron time-of-flight facility in the Center for High Power Radiation Sources of HZDR.
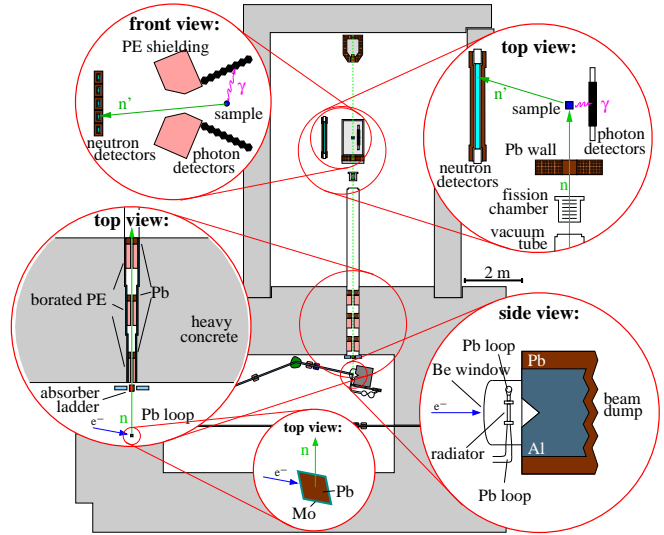

FIG. 1. Floor plan of the new nELBE neutron source and low background experimental hall.

The electron beam passes through a beryllium window mounted on a stainless-steel vacuum chamber and hits the radiator, consisting of a molybdenum channel confining the liquid lead. The channel has a rhombic cross section with 11 mm side length. The electrons generate bremsstrahlung photons which release neutrons in secondary (γ,n) reactions on lead. These leave the radiator almost isotropically, while the angular distributions of electrons and photons are strongly forward-peaked. The

---

* Corresponding author: a.junghans@hzdr.de
† Also at: Technische Universität Dresden, Dresden, Germany

collimator and the resulting neutron beam properties at the experimental area have been optimized using MCNP in order to maintain the correlation of time-of-flight and neutron energy. The collimator of 2.6 m length contains three replaceable elements of lead and borated polyethylene that are mounted inside a precision steel tube [2].

The new neutron producing target and collimator have the same design and dimensions as before the extension of the facility, consequently a very similar neutron spectrum and spatial beam profile is expected. The measurements discussed below were conducted before the facility upgrade.
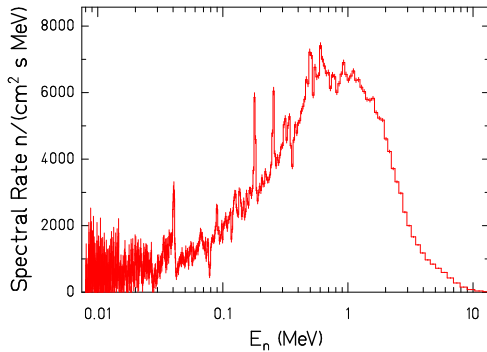

FIG. 2. Neutron spectral rate measured with the H19 fission chamber from PTB at a flight path length of 618 cm. The electron beam energy and current were 31 MeV and 15 μA, respectively.

The neutron spectral rate as shown in Figure 2, has been measured [3] with a ^{235}U fission chamber on loan from Physikalisch-Technische Bundesanstalt, Braunschweig (PTB). The time resolution of the fission chamber was estimated from the width of the photofission peak due to bremsstrahlung to be 3.8 ns (FWHM). Some absorption dips at 78, 117, 355, 528, 722, 820 keV due to scattering from resonances in ^{208}Pb can be seen. Emission peaks at 40, 89, 179, 254, 314, 605 keV are due to near threshold photoneutron emission from ^{208}Pb.

II. PHOTON PRODUCTION CROSS SECTION MEASUREMENT ^{56}FE(N,N'γ)

The inelastic scattering reaction ^{56}Fe(n,n'γ) was studied by measuring the γ-rays emitted as a function of time-of-flight. The target was a cylinder of natural iron with a diameter of 20 mm and thickness of 8 mm. An HPGe detector (60% relative efficiency) located under 125 degrees to the neutron beam and a distance of 20 cm from the target was used to measure the γ-ray energy spectrum. The time-of-flight was determined from the HPGe detector and the accelerator RF signals. A time resolution of 10 ns (FWHM) was determined from the width of the bremsstrahlung peak. The background was subtracted with the help of γ-spectra that were taken with the target out of the beam. This also helped to suppress a

possible time-of-flight uncorrelated background of γ-rays from the beta-decay to excited states of ^{56}Fe from the activation reaction ^{56}Fe(n,p)^{56}Mn. This reaction channel opens above a neutron energy of 2.966 MeV, but reaches a significant cross section only above a neutron energy of 6 MeV. Thus, only a small fraction of all neutrons contributes to this reaction.

Figure 3 shows the γ-ray energy vs. time-of-flight histogram. γ rays from excited states in ^{56}Fe are clearly visible, e.g. 847 keV, 1238 keV, and 1811 keV. To determine the inelastic scattering yield for the first few excited states the feeding from higher-lying transitions must be subtracted. This can be done, as the gamma-decay scheme is well known. The cross section was determined using the neutron spectral rate as shown in Fig. 2 including corrections for the absorption and scattering of neutrons in air and the materials in between the fission chamber and the target position, for details see Ref. [3]. From the photon production cross section under 125 degrees the angle integrated scattering cross section can be determined by Gaussian quadrature [4]. The inelastic scattering cross section for ^{56}Fe(n,n'γ) to the first 2^+, 4^+ and 6^+ states is shown in Fig. 4.

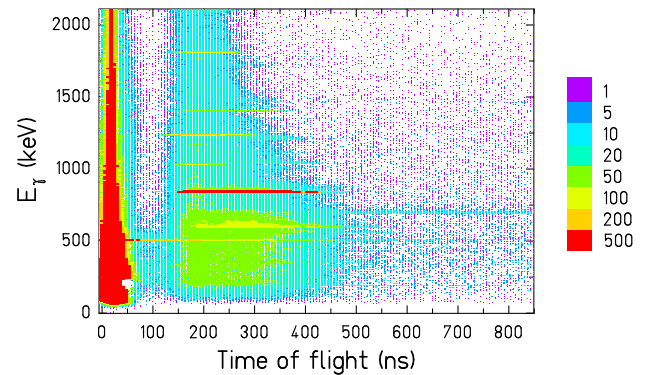FIG. 3. γ-ray energy vs. time-of-flight spectrum measured with an HPGe detector (60% relative efficiency). The absolute time-of-flight can be obtained from the bremsstrahlung peak and the flight path length.

III. TRANSMISSION MEASUREMENT OF THE NEUTRON TOTAL CROSS SECTIONS OF Au AND Ta

The target samples of Au (areal density: 0.0945(6) atoms/barn) and Ta (0.1413(6) atoms/barn) for transmission measurements together with bremsstrahlung absorbers made from PbSb4 alloy were mounted on a pneumatically driven computer-controlled target ladder directly in front of the collimator entrance. The conical neutron beam collimator has an entrance aperture diameter of 20 mm increasing to 30 mm at the exit, the target samples had a diameter of 25 mm so that all neutrons had to pass through the full target material thickness. The transmitted neutrons were detected using a plastic scintillator (Eljen EJ-200, 1000 mm x 42 mm x 11 mm)
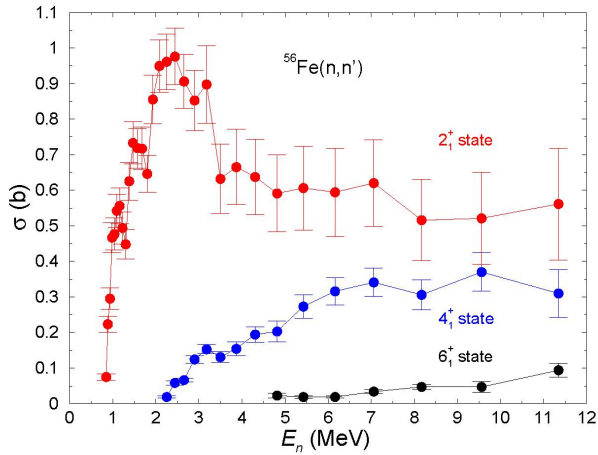
FIG. 4. Inelastic scattering cross section measurement for the first 2^+, 4^+ and 6^+ states in ^{56}Fe.

that was read out on both ends using high-gain Hamamatsu R2059-01 photomultiplier tubes. The scintillator was surrounded by a 1 cm thick lead shielding to reduce the background count rate. The detection threshold for recoil protons in this detector is at about 10 keV [5]. The
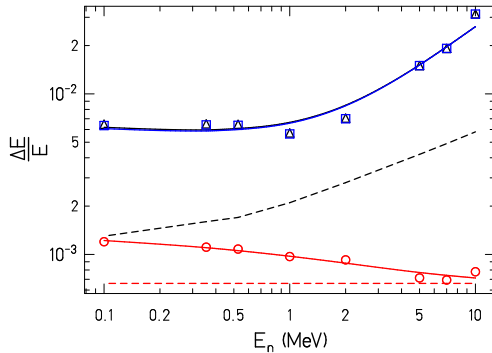

FIG. 5. Simulated neutron energy resolution (1σ) at nELBE. The resolution of the neutron source including the collimator is shown as circles with a full line in red. The resolution due to the geometrical size of the neutron radiator only is shown as a dashed red line. The energy resolution from a 1.1 cm thick plastic scintillator including a 1 cm Pb shield on all sides is shown as a blue line (squares). The square sum of source and detector resolution is shown as a black line (triangles). The dashed back line denotes the total resolution including the source and detector dimension and the detector time-of-flight resolution without neutron scattering.

target samples were periodically moved in and out of the beam to compensate possible long term drifts in the neutron beam intensity. The data taking time per cycle for the empty sample (3 cm thick PbSb4 bremsstrahlung absorber only) was 600 s, for the Au and Ta samples it was 900 s. The total measurement time was about 78 hours.

The energy resolution of the experiment was simulated

with MCNP5 for a flight path of 700 cm including the plastic scintillator and its Pb shield. The neutron energy to time-of-flight correlation can be changed by scattering of neutrons in the neutron producing target and all materials in the beam line including the collimator. Fig. 5 shows that the energy resolution is dominated by the detection system. At energies above 1 MeV the scattering of neutrons in the Pb shield close to the detector dominates the energy resolution. The simulated energy resolution was verified by the measurement of two broad resonances in ^{208}Pb at 355 keV and 527 keV, see [6].

The transmission was determined by

$$T = \frac{R_{in}}{R_{out}} = exp(-nl\sigma_{tot}) \tag{1}$$

where R_{in}, R_{out} are the background and dead-time corrected count rates in the detector with the sample in and out of the beam, respectively. The areal density is given by nl and σ_{tot} is the effective neutron total cross section that can be derived from the measured transmission data. The electron beam intensity was reduced to the sub μA range with a micropulse repetition rate of 101 kHz to have a detector count rate of 10 kHz (empty sample beam). This corresponds to a neutron count rate of approximately 250 1/s. So only about every tenth accelerator pulse is measured in the scintillator. To determine the neutron transmission and the total cross section from the measured time-of-flight distribution several corrections have to be considered [7]:

1. A time-of-flight dependent dead-time.

2. Subtraction of a constant random background in the measured time-of-flight spectra.

3. Neutron beam intensity fluctuations.

4. In-scattering of neutrons.

5. Resonant self shielding in thick transmission samples.

Random background and dead-time corrections are very important. The dead time at a pulsed neutron source is the most important correction to be made in this type of measurements, as the count rate is very different with the target sample in and out of the beam. The data acquisition dead-time was measured for each event of the listmode data acquisition system. The most probable dead time is 15 μs due to the readout times of the electronics modules used. The measured dead time per event information was used to construct a time-of-flight dependent correction factor, including source intensity fluctuations [8]. With the target out of the beam the dead-time factor was ≈ 0.575. An additional dead time of $\approx 2.7\mu$s from the constant-fraction modules of two photomultiplier signals reduced the afterpulse rate. This resulted in an additional dead-time factor of ≈ 0.96. The neutron beam intensity fluctuations were measured and found to
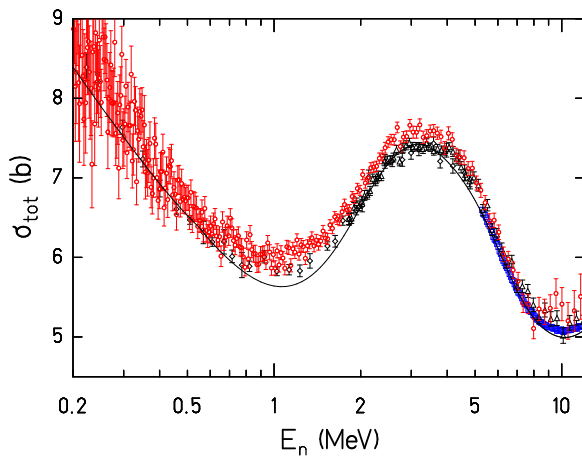
FIG. 6. Neutron total cross section of Au measured at nELBE (red circles) compared with measurements from Poenitz *et al.* [9, 10] (black diamonds, triangles) and Abfalterer *et al.* [11](blue squares). A result from the Talys code [12] is shown as a black line.

have a small influence. In-scattering of neutrons was minimized by using a "good" geometry with the transmission sample put 1 m away from the source directly in front of the collimator entrance aperture. Resonant self shielding can be an important correction at low neutron energy, where the total cross section can have strong, separated resonances, see [9]. Above 100 keV neutron energy this correction is found to be negligible.

The total systematic uncertainty including the transmission normalization (due to fluctuations of the neutron source intensity), areal density of the target samples, and the dead-time correction factor amounts to 1.1%[7]. The statistical uncertainty is shown in the error bars of Figs. 6 and 7.

The neutron total cross sections of Ta and Au have been measured in the energy range from about 0.1 MeV to 10 MeV. The energy resolution $\Delta E/E$ over this energy range increases from 1.4 % to 7.4 % (FWHM). The resolution is sufficient for average cross sections that can be compared with optical model calculations. In Fig. 6 the neutron total cross section of Au is shown in comparison with the data from Poenitz *et al.* [9, 10] and Abfalterer *et*

al. [11]. The nELBE data are systematically about 2 % higher than the data of the other two experiments. Also, our measurement extends up to the very accurate data of Abfalterer *et al.* [11] and thus demonstrates good consistency. The calculated total cross section of the Talys 1.4 code [12] shows good agreement with the data to within 4 %.

Fig. 7 shows the neutron total cross section of Ta. In the energy range from 0.2 MeV to 10 MeV our data are about 3% higher than results from Finlay *et al.* [13] and Poenitz *et al.* [9, 10] that covered only a part of this energy range. Talys does not describe the neutron total cross section correctly in the energy range below 2 MeV.
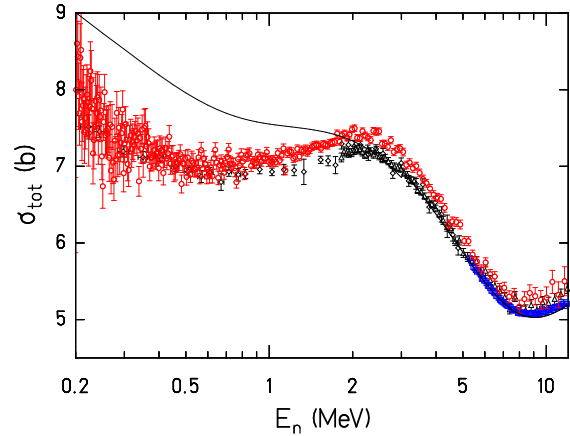

FIG. 7. Neutron total cross section of Ta measured at nELBE (red circles) compared with measurements from Poenitz *et al.* [9, 10] (black diamonds, triangles) and Finlay *et al.* [13] (blue squares). A result from the Talys code [12] is shown as a black line.

[1] E. Altstadt *et al.*, ANN. NUCL. ENERGY **34**, 36 (2007).
[2] J. Klug *et al.*, NUCL. INST. METH. **A 577**, 641 (2007).
[3] R. Beyer *et al.*, NUCL. INST. METH. **A 723**, 151 (2013).
[4] L.C. Mihailescu *et al.*, NUCL. INST. METH. **A 531**, 375 (2004).
[5] R. Beyer *et al.*, NUCL. INST. METH. **A 575**, 449 (2007).
[6] P. Schillebeeckx *et al.*, NUCL. DATA SHEETS **113**, 3054 (2012).
[7] R. Hannaske,*et al.*, subm. to EUR. PHYS. JOUR. **A** (2013).
[8] M. Moore, NUCL. INST. METH. **169**, 245 (1980).
[9] W. Poenitz, J. Whalen and A. Smith, NUCL. SCI. ENG. **78**, 333 (1981).
[10] W. Poenitz and J. Whalen, Report ANL/NDM-80 (1983).
[11] W. P. Abfalterer *et al.*, PHYS. REV. **C 63**, 044608 (2001).
[12] A.J. Koning *et al.*, Proc. Int. Conf. Nucl. Data for Science and Tech., Nice, France, 2007, EDP Sciences 2008, 211.
[13] R. W. Finlay *et al.*, PHYS. REV. **C 47**, 237 (1993).